Am J Cancer Res 2021;11(6):3163-3175
www.ajcr.us /ISSN:2156-6976/ajcr0130174

Original Article

Dysbiotic gut microbiota in pancreatic cancer patients form correlation networks with the oral microbiota and prognostic factors

Hiroki Matsukawa[1*], Noriho Iida[1*], Kazuya Kitamura[1], Takeshi Terashima[1], Jun Seishima[1], Isamu Makino[2], Takayuki Kannon[3], Kazuyoshi Hosomichi[3], Taro Yamashita[1], Yoshio Sakai[1], Masao Honda[4], Tatsuya Yamashita[1], Eishiro Mizukoshi[1], Shuichi Kaneko[1]

[1]Department of Gastroenterology, Graduate School of Medical Sciences, Kanazawa University, 13-1 Takara-Machi, Kanazawa, Ishikawa, Japan; [2]Department of Hepato-Biliary-Pancreatic Surgery and Transplantation, Graduate School of Medical Sciences, Kanazawa University, 13-1 Takara-Machi, Kanazawa, Ishikawa, Japan; [3]Department of Bioinformatics and Genomics, Graduate School of Advanced Preventive Medical Sciences, Kanazawa University, 13-1 Takara-Machi, Kanazawa, Ishikawa, Japan; [4]Department of Advanced Medical Technology, Graduate School of Health Medicine, Kanazawa University, 13-1 Takara-Machi, Kanazawa, Ishikawa, Japan. [*]Equal contributors.

Received January 15, 2021; Accepted March 17, 2021; Epub June 15, 2021; Published June 30, 2021

Abstract: Microbiota in the gut and oral cavities of pancreatic cancer (PC) patients differ from those of healthy persons, and bacteria in PC tissues are associated with patients' prognoses. However, the species-level relationship between a dysbiotic gut, oral and cancerous microbiota, and prognostic factors remains unknown. Whole-genome sequencing was performed with fecal DNA from 24 PC patients and 18 healthy persons (HD). Microbial taxonomies, metabolic pathways, and viral presence were determined. DNA was sequenced from saliva and PC tissues, and the association between the gut, oral, and cancer microbiota and prognostic factors in PC patients was analyzed. The PC microbiota were altered from those of the healthy microbiota in terms of microbial taxonomy, pathways and viral presence. Twenty-six species differed significantly between the PC and HD microbiota. Six fecal microbes, including *Klebsiella pneumoniae*, were associated with an increased hazard of death. In the co-occurrence network, microbes that were abundant in PC patients were plotted close together and formed clusters with prognosis-associated microbes, including *K. pneumoniae*. Multiple salivary microbes were present in the co-occurrence network. *Microbacterium* and *Stenotrophomonas* were detected in the PC tissues and formed a network with the fecal and salivary microbes. The dysbiotic gut microbiota in the PC patients formed a complex network with the oral and cancerous microbiota, and gut microbes abundant in the PC patients were closely linked with poor prognostic factors in the network.

Keywords: Metagenome, virome, microbiome, prognosis, ductal adenocarcinoma

Introduction

Pancreatic cancer (PC) incidence is increasing, and PC is currently the fourth leading cause of cancer-related death worldwide [1]. The prognosis of patients with PC is generally poor with a 5-year overall survival rate of 9% [1]. One reason for the poor prognosis is the difficulty of diagnosing PCs in the early stages. Known risk factors for PC are limited to age, obesity, chronic pancreatitis and hereditary PC syndrome [2], and most PC cases are diagnosed without obvious risks. Even when patients undergo surgical resection of PCs, the median overall survival time is as short as 24-30 months owing to high recurrence rates [1]. Thus, diagnostic markers for early detection and prognostic markers to help determine appropriate treatments are necessary to improve PC patient prognoses.

Recent clinical and preclinical studies highlight the emerging roles of the microbiota in patients with PCs. Several studies demonstrated the presence of multiple microbes in PC tissues

[3-5]. Specific groups of microorganisms in cancer tissues correlate with cancer patients' prognoses [3]. A preclinical model of PCs revealed some of the mechanisms underlying the relationship between PC tissues and the cancer microbiota. Roles of the cancer microbiota in suppressing anticancer immunity [5], metabolism of anticancer drugs [4], and carcinogenesis [5, 6] were substantiated in a mouse model. Therefore, bacterial presence in PC tissues might be a good biomarker for treatment selection or a prognostic marker for predicting treatment effects; however, bacterial presence cannot be a diagnostic marker for cancer. Conversely, several hypotheses have proposed that the intestinal or oral microbiota are possible origins of bacteria in PC tissues [7]. The oral microbiota can reach the pancreas via reflux to the pancreatic duct from the duodenum, while the fecal microbiota might translocate to the pancreas through the portal circulation or mesenteric lymph nodes [7]. Several studies reported that the relative abundance of multiple bacterial genera in the gut and saliva differed between PC patients and healthy controls [5, 8, 9]. A direct comparison of the gut and cancer microbiomes in PC patients via 16S rRNA-sequencing data showed that the Proteobacteria phylum was translocated from the gut to the pancreas [5, 10]. Thus, detection of specific fecal or salivary microorganisms, rather than the cancer microbiota, may be a non-invasive biomarker for early diagnosis or prognostic prediction. However, past studies adopted 16S rRNA-based sequencing to detect genus-level fecal bacteria [5, 8], and which species are abundant in the gut and oral cavities of PC patients and how intestinal and oral bacterial species are associated with cancer bacteria and prognosis remain unknown.

Here, we performed whole-genome sequencing of fecal and salivary DNA from PC patients to determine the species-level microbial compositions. The subsequent analyses revealed characteristics of the microbiomes and viromes in the guts of patients with PC and the relationship between the intestinal, oral, and cancer microbiota and the clinical characteristics of these patients.

Materials and methods

Clinical study population

The study population comprised 24 PC patients admitted to Kanazawa University Hospital between August 2014 and September 2019 who received written and oral information before consenting to participate. PC was pathologically diagnosed from aspiration biopsy specimens. If a patient underwent surgical resection, the diagnosis was also confirmed from the surgically resected specimens. The diagnoses included 22 pancreatic ductal adenocarcinomas, 1 intraepithelial neoplasia and 1 adenocarcinoma accompanied by an intraductal papillary mucinous neoplasm. The PC stage was determined per the Union for International Cancer Control Tumor Node Metastasis system. All 24 patients had primary PCs (no recurrent cancers) and received anticancer treatment after enrollment. All participants were followed until July 2020 to monitor overall survival. Fecal or salivary samples were collected and stored at -80°C immediately after enrollment to investigate the gut and oral microbiota compositions.

Healthy volunteers were tested to determine whether they met the inclusion criteria: body mass index <25 kg/m^2, normal blood pressure, normal serum cholesterol levels, normal blood glucose and HbA1c levels, normal serum aspartate aminotransferase (AST) and alanine aminotransferase (ALT) levels, no anemia, no fatty liver in ultrasonography, and no past history of cancer. Eighteen persons passed the criteria and were enrolled as healthy sample donors (HDs). The Ethics Committee of Kanazawa University approved the study (approval number 2012-109).

Whole-genome sequencing of fecal and salivary DNA

Fecal DNA was extracted from the feces that had been stored at -80°C using the PowerFecal DNA Isolation Kit per the manufacturer's instructions with slight modifications (QIAGEN, Limburg, Germany). Beads to homogenize the feces were changed from 0.7 mm garnet beads to 0.1 mm glass beads (QIAGEN). After centrifugation of 1 ml of saliva at 3,300×g for 10 min, pellets were similarly used to extract the salivary DNA.

For whole-genome sequencing, tagmentation of DNA was performed with the Nextera DNA Flex Library Prep Kit (Illumina, San Diego, CA, USA) by reaction at 55°C for 15 min. After cleaning the products, indexing PCR was per-

formed using the Nextera DNA CD Index Kit (Illumina) with an initial step at 68°C for 3 min and 98°C for 3 min, followed by 5 cycles of 45 sec at 98°C, 30 sec at 62°C and 2 min at 68°C. PCR products were purified from sample purification beads in the Nextera kit and quantified using a 2100 Bioanalyzer and High-Sensitivity DNA Kit (Agilent Technologies, Santa Clara, CA, USA). The libraries were pooled and sequenced with a MiSeq instrument using the MiSeq Reagent Kit V3 (600 cycles; Illumina).

The acquired sequences were preprocessed as follows. After trimming bases with low-quality scores from the ends of the acquired sequences, the sequences were filtered with a Q-score cut-off of 20 by FASTX Toolkit [11]. Paired-end joining was performed using MacQIIME v1.9.1 [12]. After mapping the resultant sequences on The University of California, Santa Cruz (UCSC) human genome reference hg19 using bowtie2 version 2.2.4 [13], human genome sequences were removed by SAMtools-1.2 [14]. Finally, PCR duplicates were removed using PRINSEQ version 0.20.4 [11].

The final output fasta files were used to identify taxonomies in the fecal samples using MetaPhlAn2 version 2.0.0 [15]. Metabolic pathways in the sequences were also analyzed with the fasta files using HUMAnN2 [16]. The Kyoto Encyclopedia of Genes and Genomes (KEGG) version 56 database was generated using DIAMOND version 0.7.5 [17] and used for HUMAnN2 analysis. Eukaryotic viruses from fecal DNA sequences were detected and profiled via ViromeScan [18]. After normalizing the abundance by 1 million reads, groups were compared by linear discriminant analysis using LefSe [19]. Bray-Curtis dissimilarities of the gut microbiota communities were calculated based on taxonomy or metabolic pathway data, and the resultant distances were visualized by principal coordinate analysis (PCoA). Statistical differences between communities were tested by PERMANOVA.

All whole-genome sequencing data and metadata were archived in NCBI SRA as BioProject PRJNA665854.

16S ribosomal RNA amplicon sequencing of tumor DNA

Tumor DNA was extracted as previously described [3]. Three sections of 10-μm formalin-fixed paraffin-embedded (FFPE) PC tissue were aseptically collected and placed in 1.5 ml tubes. Paraffin without tissues was used as a negative control for DNA extraction. Genomic DNA was extracted using the QIAGEN QIAamp DNA FFPE kit (QIAGEN). For 16S sequencing analysis, PCR amplicons were prepared using primers [20, 21] consisting of sequences targeting the V3-V4 regions of the 16S rRNA and Illumina adapter overhang nucleotide sequences as follows: Forward 5'-TCGTCGGCAGCGTCAGATGTGTATAAGAGACAGCCTACGGGNGGCWGCAG-3'; Reverse 5'-GTCTCGTGGGCTCGGAGATGTGTATAAGAGACAGGACTACHVGGGTATCTAATCC-3'.

PCR was performed using KAPA HiFi HotStart Ready Mix (KAPA Biosystems, Wilmington, MA, USA) with an initial step at 95°C for 3 min, followed by 25 cycles of 30 sec at 95°C, 30 sec at 55°C and 30 sec at 72°C and a final step at 72°C for 5 min. After purification, indexing PCR was performed using the Nextera XT Index Kit (Illumina) with an initial step at 95°C for 3 min, followed by eight cycles of 30 sec at 95°C, 30 sec at 55°C and 30 sec at 72°C and a final step at 72°C for 5 min. The libraries were pooled and mixed with the PhiX control library (Illumina) and sequenced in a MiSeq instrument with the MiSeq Reagent Kit V3 (600 cycles; Illumina). Downstream sequences were processed using MacQIIME v1.9.1 [12]. Operational taxonomic units (OTUs) were picked using UCLUST [22]. For OTU analysis, the sequences were clustered, and sequences with >97% similarity were binned into the same OTUs. Representative sequence taxonomies in the OTUs were assigned via RDP Classifier using the Greengenes reference database [23] clustered at 97% identity. Genus-level taxonomy was summarized and used for subsequent analysis.

All 16S rRNA amplicon sequencing data and metadata were archived in NCBI SRA as BioProject PRJNA665618.

Survival, correlation and network analysis

The hazard ratio for death was calculated using overall survival data from the PC patients since the study enrollment. Cox proportional hazard models were used with SPSS Statistics v25.0.0.2 (IBM, Armonk, NY, USA). Spearman correlation between clinical factors, relative abundances of fecal or salivary microbes, fecal microbial pathways, and fecal viruses were cal-

culated with SPSS Statistics v25.0.0.2. Pearson correlation was calculated between the relative abundances of fecal, salivary and tumor microbes in PC patients and shown as networks using Cytoscape v3.8.0 [24] with MetScape plugin [25]. Correlations coefficients ≥0.7 are shown as edges.

Statistical analyses

Statistical analyses for comparing taxonomy and KEGG pathways between microbial communities were performed using linear discriminant analysis with a LEfSe tool [19]. Statistical differences between two values were analyzed via the Mann-Whitney U test with GraphPad Prism 7 (GraphPad, San Diego, CA, USA). Statistical differences in the baseline characteristics were analyzed using χ^2 tests in GraphPad Prism 7.

Spearman's correlation coefficients and Cox proportional hazards were calculated using SPSS.

$P<0.05$ was considered statistically significant.

Data availability

All whole-genome sequencing data and metadata were archived in NCBI SRA as BioProject PRJNA665854. All 16S rRNA amplicon sequencing data and metadata were archived in NCBI SRA as BioProject PRJNA665618.

Results

Gut microbiota of PC patients were taxonomically and functionally altered compared with those of HDs

Feces from 18 HDs and 24 PC patients were collected to investigate the taxonomic and functional differences in gut microbiota between patients with PC and HDs. Plasma glucose concentrations and glycated hemoglobin A1c were higher in the PC patients than in the HDs (Supplementary Table 1), as occupation of pancreatic tissues by PC impaires function of insulin secretion. Utilization rates of gastric acid-reducers, including proton-pump inhibitors (PPIs) and H2 receptor antagonists (H2RAs), were higher in PC patients than in the HDs, because no HDs used PPIs/H2RAs (Supplementary Table 1). PC patients were in various stages of the cancer, ranging from stage 0 (intraepithelial neoplasia) to stage 4 (Supplementary Table 1). Whole-genome sequencing of the fecal DNA was performed and microbiota taxonomies, pathways included in the microbiota genomes, and viral presence were determined. Bray-Curtis dissimilarity results between the fecal microbiota of the 42 subjects revealed that the PC microbiota differed taxonomically compared with the HD microbiota (P=0.001 by PERMANOVA; **Figure 1A**). Twenty-six species differed significantly between the PC patients and HDs. *Klebsiella pneumoniae*, *Clostridium bolteae*, *C. symbiosum*, *Streptococcus mutans*, *Alistipes shahii*, 4 *Bacteroides* species, 2 *Parabacteroides* species, and 2 *Lactobacillus* species were significantly more abundant in the PC microbiota than in the HD microbiota (**Figure 1B**). Analysis of microbial pathway-based dissimilarity showed that the PC microbiota differed from the HD microbiota (P=0.001 by PERMANOVA; **Figure 1C**). Forty-four KEGG metabolic pathways differed significantly between the patients and HDs. The PC-abundant pathways included several carbohydrate metabolism-related and glycan metabolism-related pathways containing lipopolysaccharide biosynthesis (Supplementary Table 2). Viral sequences in the fecal DNA and viral genera were also determined. The PC gut virome also differed from the HD virome based on analysis of virus-based dissimilarity (P=0.021 by PERMANOVA; **Figure 1D**). Nineteen viral genera differed significantly between the patients and HDs (**Figure 1E**).

Because gastric acid-reducers affect the gut microbiota composition [26-28], we compared HDs and PC patients who had not received PPIs or H2RAs to exclude the effects of these drugs on the gut microbial composition. The microbiota of 14 subjects with PC without PPI/H2RA treatment still differed significantly from the HD microbiota based on taxonomy-based dissimilarity (P=0.007 by PERMANOVA; Supplementary Figure 1A). Relative abundances of 17 bacterial species differed significantly between the groups (Supplementary Figure 1B). Furthermore, the abundances of nine species differed significantly between PPI/H2RA-treated PC patients and PPI/H2RA-untreated patients. PPI/H2RA use was associated with increased relative abundances of seven species: *S. salivarius*, *S. parasanguinis*, *S. anginosus*, *Bifidobacterium dentium*, *Veillonella par-*

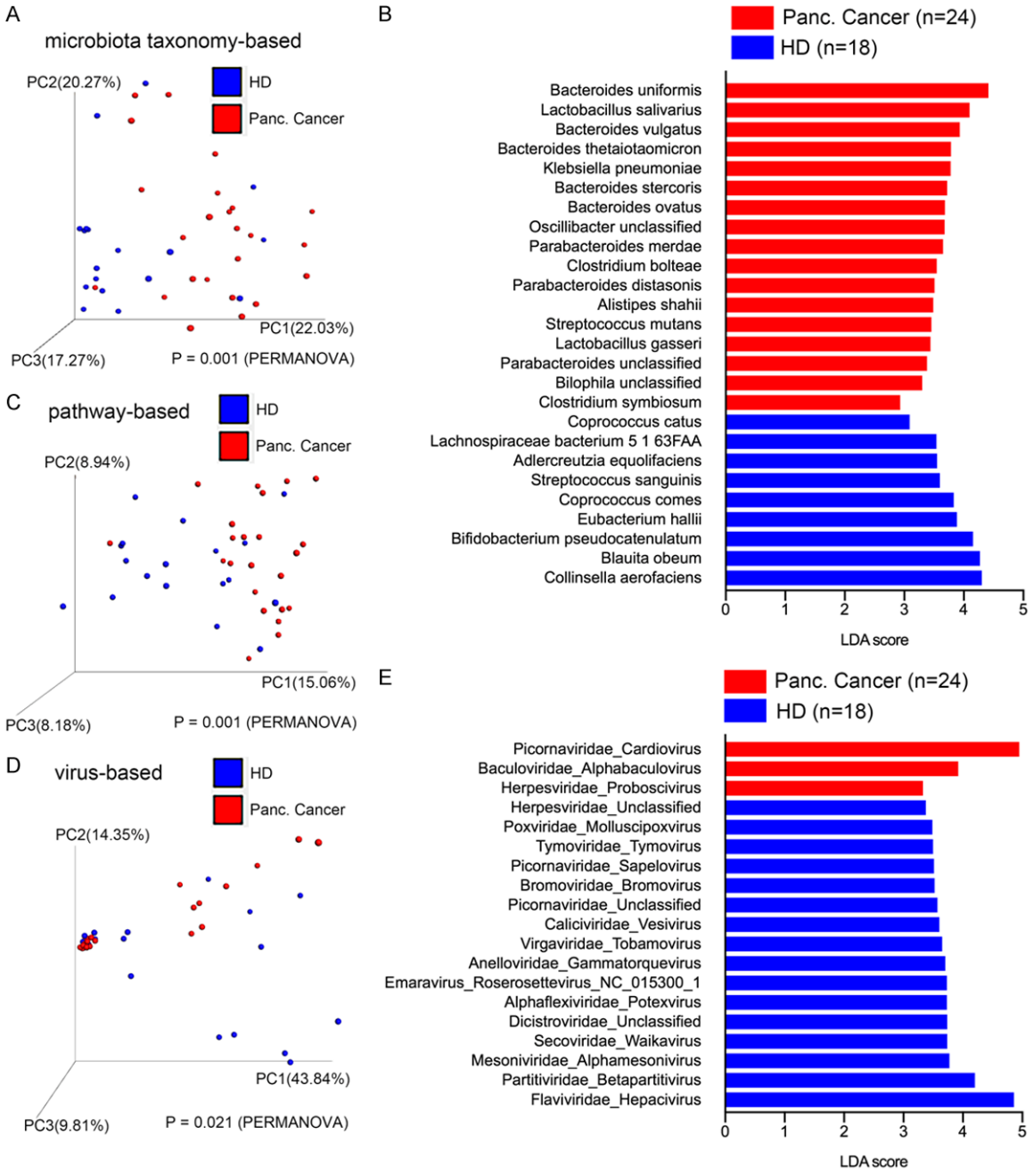

Figure 1. Fecal microbiomes and viromes of pancreatic cancer patients are altered from those of healthy subjects. Distances between fecal samples were calculated using the Bray-Curtis index based on microbial taxonomy data (A), microbial pathway data (C), or viral genus data (D) and shown as PCoA plots. Linear discriminant analysis (LDA) was performed using LDA effect size (LEfSe) to identify significant differences in relative abundances of various microbial taxonomies (B) or viral genera (E) in the fecal samples. Differentially abundant taxonomies are indicated by the corresponding LDA scores (P<0.05).

vula, *Lactobacillus fermentum* and *Lactobacillus gasseri* (Supplementary Figure 1C). Thus, these 7 species were considered PPI/H2RA-associated species. Because blood glucose concentrations were higher in the patients than in the HDs according to the baseline characteristics (Supplementary Table 1), we compared HDs and PC patients with normal HbA1c levels to exclude hyperglycemic effects on the gut microbial composition. Twenty-one species,

Table 1. Prognostic factors in pancreatic cancer patients

Factors	Univariate *P*-value	Hazard ratio of death	Multivariate *P*-value
cancer stage	0.026	3.646	0.962
serum CEA (mg/dl)	0.018	1.979	0.884
PPI/H2RA (medicated)	0.049	8.715	0.874
feces_Bifidobacterium animalis	0.012	1.650	0.989
feces_Collinsella aerofaciens	0.018	2.455	0.913
feces_Eubacterium ventriosum	0.009	71.33	0.730
feces_Klebsiella pneumoniae	0.046	1.117	0.703
feces_Roseburia intestinalis	0.030	62.76	0.856
feces_Streptococcus thermophilus	0.022	3.286	0.900

CEA, carcinoembryonic antigen; H2RA, H_2 receptor antagonist; PPI, proton-pump inhibitor.

Table 2. Factors correlated with serum CEA

Factors	Correlation coefficient	*P*-value
cancer stage	0.629	0.012
feces_Bacteroides stercoris	0.662	0.007
feces_Clostridium bolteae	0.604	0.017
feces_Dorea longicatena	-0.630	0.012
saliva_Gemella haemolysans	0.597	0.019

including *K. pneumonia*, *C. bolteae*, *S. mutans*, 6 *Bacteroides* species and 2 *Parabacteroides* species, were significantly more abundant in the patients than in the HDs even after excluding 10 PC patients with high HbA1c (Supplementary Figure 1D). Only two species (*Bifidobacterium bifidum* and *Bifidobacterium breve*) were more abundant in the microbiota of patients with high HbA1c than in those of patients with normal HbA1c (Supplementary Figure 1E).

PC microbiota were dysbiotic in terms of microbial taxonomy, pathways and viral presence compared with those of the HD microbiota. This dysbiosis might be related to the presence of PC. The effects of PPIs/H2RAs and hyperglycemia on the gut microbiota compositions were limited.

Gut microbes abundant in PC patients formed networks with the oral microbiota and prognosis-associated microbes

The hazard ratio for death in various factors was analyzed via Cox proportional hazard models to determine whether microbes and viruses that were abundant in PC patients were associated with patient prognoses. Saliva was obtained from 15 of 24 PC patients, and their salivary microbiota were determined by whole-genome sequencing. Because treatments provided to the PC patients were varied and combinational (Supplementary Table 3), we analyzed cancer stage, rather than treatment, as a possible prognostic factor. In the univariate analysis, cancer stage, serum carcinoembryonic antigen (CEA) concentrations, PPI/H2RA use, relative abundances of fecal *Bifidobacterium animalis*, *Collinsella aerofaciens*, *Eubacterium ventriosum*, *K. pneumoniae*, *Roseburia intestinalis* and *S. thermophilus* were associated with an increased hazard ratio for death (**Table 1**). Conversely, no viruses, microbial pathways, or salivary microbes were significantly associated with the hazard ratio of death (Supplementary Table 4). However, multivariate analysis showed that none of those nine factors were independently associated with the hazard ratio of death (**Table 1**); therefore, the factors may have been confounders. Correlation analysis was performed for cancer stage and serum CEA, both of which were positively associated with an increased hazard ratio of death, to find confounding factors for cancer stage and serum CEA. Serum CEA level was positively correlated with cancer stage and relative abundance of two fecal bacterial species, *Bacteroides stercoris* and *C. bolteae*, and salivary *Gemella haemolysans* (**Table 2**). Cancer stage was positively correlated with relative abundances of fecal *Alistipes purtredinis* and Cyprinivirus and three salivary species, Human herpesvirus 4 (Epstein-Barr virus), *Lachnospiraceae bacterium*, and *Leptotrichia wadei* (**Table 3**). To clarify relationships between these prognosis-related microbes and the microbes abundant in PC, co-occurrences of fecal and salivary microbes were calculated via Pearson's correlation analysis and visualized by networking (Supplementary Figure 2 and **Figure 2**). In the co-occurrence network, microbes abundant in PC were closely plotted and formed two clusters. The "*K. pneumoniae* cluster" contained 7 microbes abundant in PC: *K. pneumoniae*,

Table 3. Factors correlated with cancer stage

Factors	Correlation coefficient	*P*-value
serum CEA	0.629	0.012
feces_Alistipes putredinis	0.546	0.035
feces_Bifidobacterium adolescentis	-0.528	0.043
saliva_Human herpesvirus 4	0.523	0.045
saliva_Lachnospiraceae bacterium (oral taxon 082)	0.523	0.045
saliva_Leptotrichia wadei	0.523	0.045
feces_Alloherpesviridae; Cyprinivirus	0.667	0.007

Bacteroides stercoris, *Bacteroides vulgatus*, *Bacteroides uniforms*, *Bacteroides ovatus*, *C. symbiosum* and *Parabacteroides merdae*. In this cluster, *K. pneumonia* and *Roseburia intestinalis* were associated with an increased hazard of death, and *Bacteroides stercoris* was positively correlated with CEA level (**Figure 2**). The "*C. bolteae* cluster" contained 4 microbes abundant in PC: *C. bolteae*, *Bacteroides thetaiotaomicron*, *S. mutans*, and *Parabacteroides distasonis*. *C. bolteae* was positively correlated with CEA level (**Figure 2**). In the intermediate position of these 2 clusters, many salivary microbes were plotted and formed "Salivary microbe clusters". In this cluster, 2 salivary bacterial species, *Leptotrichia wadei* and *Lachnospiraceae bacterium*, and human herpesvirus 4 correlated positively with cancer stage (**Figure 2**). Thus, gut microbes abundant in PC formed networks with prognosis-related, stage-related and CEA-related microbes and formed complex networks with the oral microbiota.

Microbes in PC tissue formed co-occurrence networks with fecal and oral microbes

Because microbes in PC tissues are associated with cancer patient prognoses and anticancer treatment effects [3-5], we collected PC tissues from seven patients who had undergone surgery from the 24 PC patients and determined microbes in the cancer tissues via 16S rRNA-amplification sequencing. Ten microbial taxonomies were detected in the PC tissues (Supplementary Figure 3). *Microbacterium* and *Stenotrophomonas* presence in PC tissues has been previously reported [3, 5], and both genera were significantly abundant in the PC patients compared with those of the paraffin controls (**Figure 3A**). Both cancer *Microbacterium* and *Stenotrophomonas* formed co-occurrence networks with fecal and salivary microbes (**Figure 3B** and Supplementary Figure 2). Four fecal microbes associated with poor survival (*S. thermophiles*, *Bifidobacterium animalis*, *Eubacterium ventriosum* and *Collinsella aerofaciens*) formed a cluster, but it was not close to the cancer microbes (**Figure 3B**). Rather, the cancer *Stenotrophomonas* was strongly positively correlated with fecal *Bifidobacterium adolescentis*, which was negatively correlated with cancer stage (**Figure 3B** and **Table 2**).

In summary, dysbiotic gut microbiota in PC patients formed complex networks with the oral and cancer microbiota, and gut microbes abundant in the PC patients were closely linked with poor prognostic factors in the network.

Discussion

Detailed species-level compositions of the dysbiotic gut microbiota of PC patients and associations of the gut microbiota with oral or cancer microbiota remain unknown. We performed species-level comparisons of the dysbiotic gut microbiota of PC patients and HDs via whole-genome sequencing (**Figure 1A** and **1B**). Microbial pathways and viromes in the guts of the PC patients differed from those of the HDs (**Figure 1C-E**). The dysbiosis was attributed to the presence of cancer tissues in the pancreas, while the effects of PPIs/H2RAs or hyperglycemia on the gut microbial composition were limited. Gut microbes abundant in PC formed co-occurrence networks with both oral-cavity and prognosis-associated microbes (**Figure 2**). Notably, *K. pneumonia*, a PC-abundant gut microbe, was associated with an increased hazard ratio of death (**Table 1**) and formed a cluster with other PC-abundant gut microbes and CEA-correlated microbes (**Figure 2** and **Table 2**). *Microbacterium* and *Stenotrophomonas* were detected in PC tissues and formed a co-occurrence network with the gut and oral microbiota (**Figure 3**). Thus, gut microbiota dysbiosis occurred in PC patients in this cohort, and the microbiota formed complex networks with the oral microbiota and prognosis-related factors.

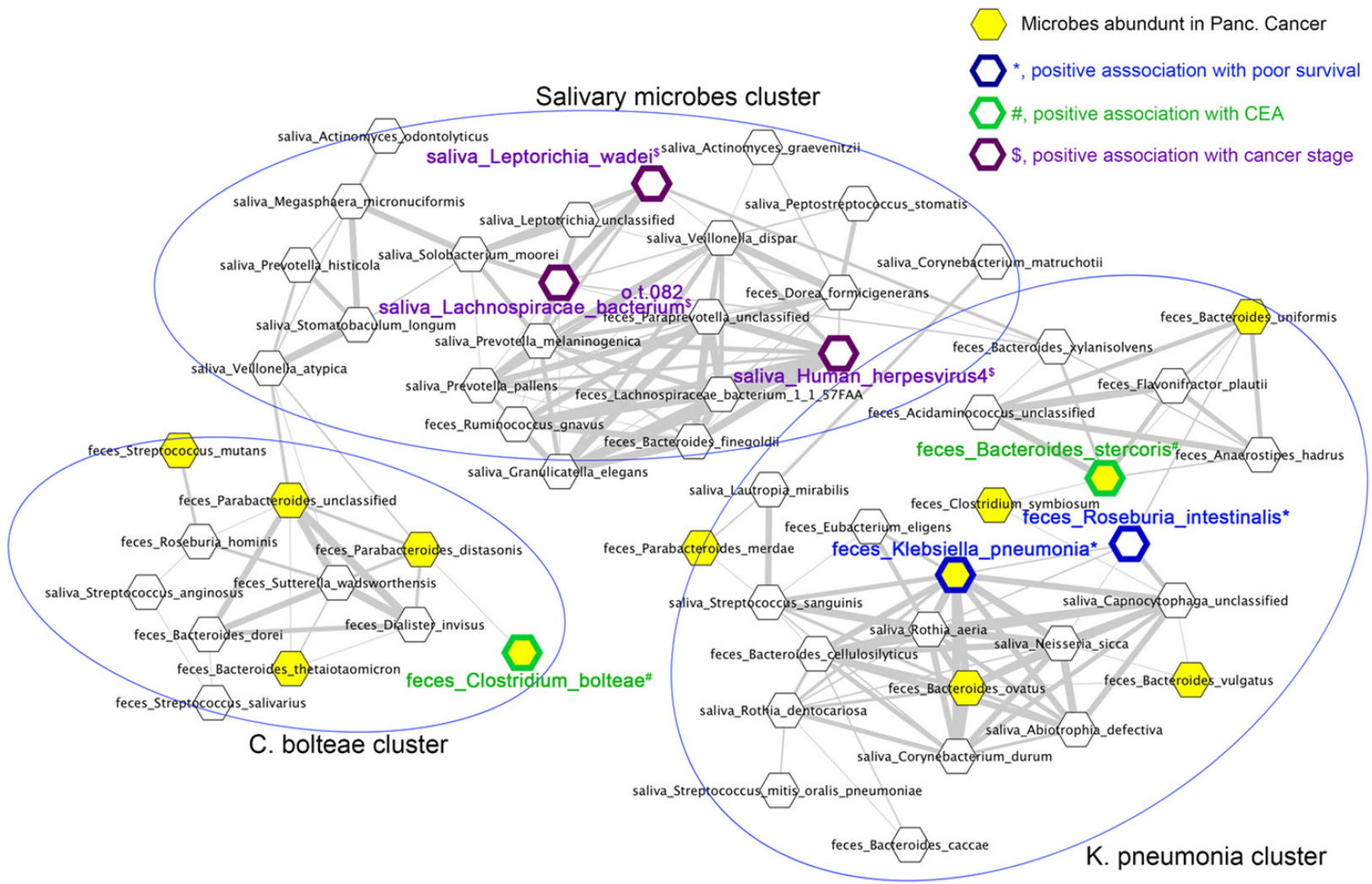

Figure 2. Gut microbiota compositions of pancreatic cancer patients are highly associated with the oral microbiota and prognostic factors. Pearson correlation was calculated between relative abundances of fecal and salivary microbes in PC patients and is shown as networks. Correlations coefficients ≥0.7 are shown as edges. Nodes of fecal microbes abundant in PC patients compared with HDs are highlighted in yellow. *, positive association with a poor prognosis based on the increased hazard of death, blue border; #, positive association with serum CEA level, green border; $, positive association with cancer stage, purple border. This figure is part of Supplementary Figure 2.

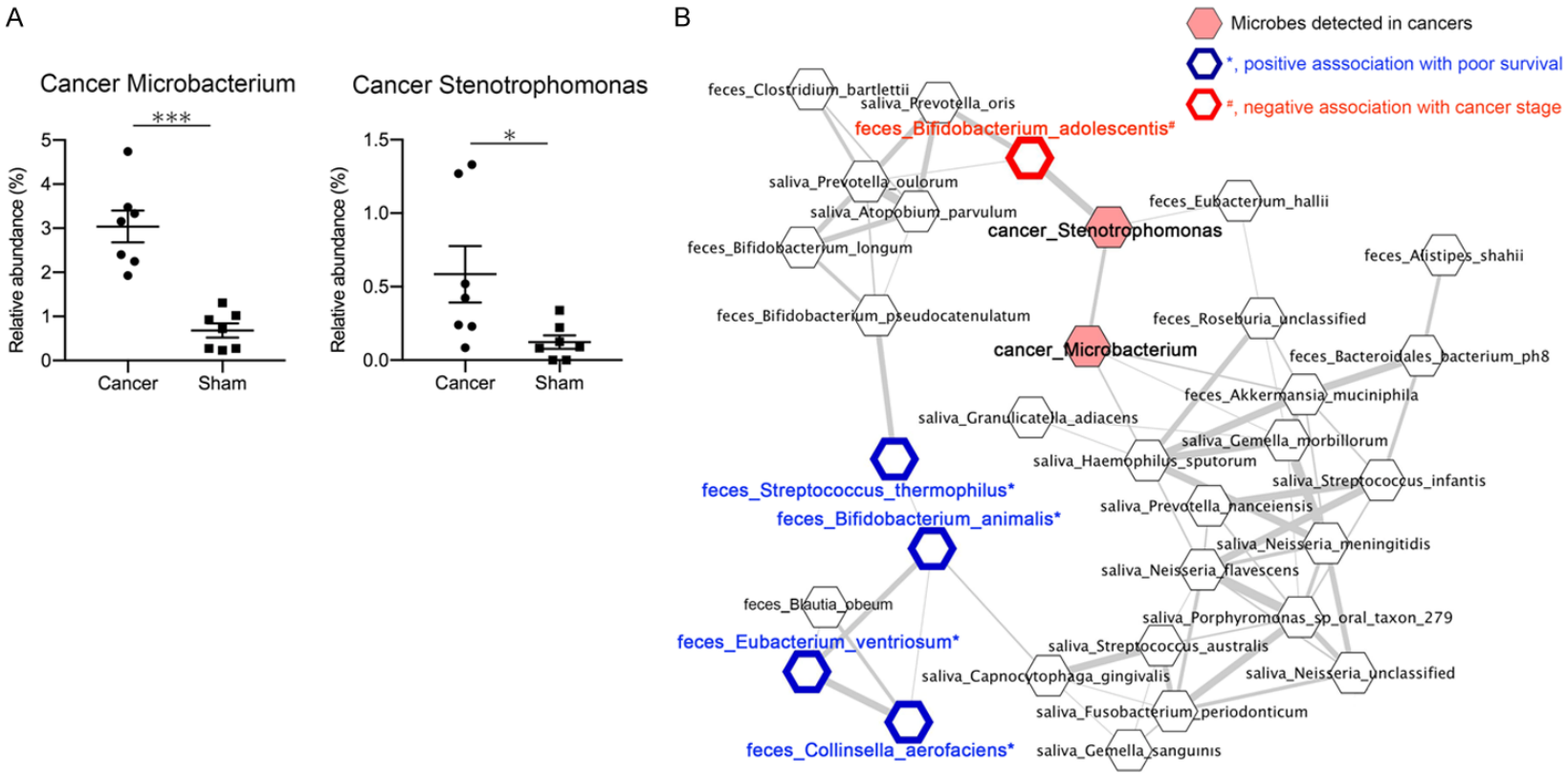

Figure 3. Microbes in pancreatic cancer tissue form co-occurrence networks with fecal and oral microbes. A. Relative abundances of *Microbacterium* (left) and *Stenotrophomonas* (right) in pancreatic cancer tissues or sham paraffin controls. *, $P<0.05$; ***, $P<0.001$. B. Pearson correlation was calculated between relative abundances of fecal, salivary, and cancer microbes in PC patients and shown as networks. Correlations coefficients ≥0.7 are shown as edges. Nodes of cancer microbes are highlighted in pink. *, positive association with poor prognosis based on the increased hazard of death, blue border; #, negative association with cancer stage, red border. This figure is part of Supplementary Figure 2.

The number of the subjects in this study was relatively low compared with the previous 16S rRNA-based studies [3, 5]. Differences in age and serum CRP level between HD and PC were not significant, but not small, so they needed to be taken in consideration for interpretation of results. However, this study performed whole-genome sequencing-based identification of bacterial species, viral genera and metabolic pathway in feces and saliva unlike 16S rRNA-based analysis in the previous reports. 16S rRNA-based analysis could only identify genus-level microbiota, but whole-genome-based analysis identifies species-level microbiota. Therefore, species-based analysis in this study enabled us to obtain the more detailed analysis regarding difference between HD and PC patients and the correlation to the prognosis. In addition, relationship between feces, saliva and cancer microbiota was not analyzed in the previous study, and the current study clarified networks between microbiota in feces, saliva and cancer.

Mechanisms underlying the effects of the gut microbiota on cancer patient prognoses remain unclear. Several preclinical models and observations in patients revealed that gut microbiota are related to systemic inflammation, including inflammation in tumors. Mouse models of subcutaneous melanoma and colon cancer demonstrated that gut microbiota are necessary to increase inflammatory responses in tumors [29].

Microbiota-depleted mice showed decreased inflammatory and immune-related gene expressions in the tumors and a decreased inflammatory myeloid cell population in the tumor microenvironment. Oral gavage with *Alistipes shahii* in microbiota-depleted mice restored tumor inflammation [29]. In this study, *Alistipes shahii* was abundant in the feces of PC patients, although a role of *Alistipe*s in humans remains unknown. In hepatocellular carcinoma patients, use of anti-anaerobic drugs is associated with a poor prognosis after chemotherapy and several anaerobic microbes are positively associated with prolonged survival and negatively associated with systemic inflammatory markers such as white blood cell counts and C-reactive protein [30]. Conversely, intestinal *Microbacterium* and *Enterococcus* are positively associated with systemic inflammatory markers [30].

One cause of systemic inflammation is translocation of bacteria or bacterial products into the circulation. The gut microbiota may translocate to pancreatic tissues via the portal circulation or mesenteric lymph nodes [7]. For gut microbes to enter the circulation, a disruption of the gut barrier and increased gut permeability are required. Because gut microbes control the gut barrier function [31-33], composition of the gut microbiota is closely associated with gut permeability. A monolayer culture of intestinal organoids revealed that *K. pneumoniae* increases gut permeability by inducing epithelial pore structures [34]. *K. pneumoniae* invades the colonic epithelia and promotes inflammatory bowel disease [35] and primary sclerosing cholangitis [34]. *Klebsiella* was abundant in the fecal microbiota of pancreatic ductal adenocarcinoma patients of two independent cohorts [5, 8]. Thus, one possible mechanism underlying the association between a dysbiotic gut microbiota and a poor prognosis for PC patients might be the gut barrier disruption and subsequent bacterial translocation induced by dysbiotic microbes, including *K. pneumoniae*.

Metagenomic analysis revealed the presence of a cancer microbiota in PC patients in 2017 [4]. Cancer microbiota usually include Proteobacteria, Firmicutes and Actinobacteria, whereas obligate anaerobes, such as Bacteroidetes, are rarely detected [3, 4]. Roles of cancer bacteria have been substantiated by preclinical models and culture experiments. *K pneumoniae* and *Escherichia coli* metabolize the cytotoxic drug, gemcitabine. Deleting *E. coli* via ciprofloxacin increased the anticancer effects of gemcitabine in a mouse cancer model [4]. Cancer bacteria also induce tolerogenic monocytic cells via Toll-like receptor signaling and suppress differentiation of Th1-type $CD4^+$ T cells and cytotoxic $CD8^+$ T cells in the tumor microenvironment [5]. In pancreatic ductal adenocarcinoma patients, presence of *Pseudoxanthomonas*, *Streptomyces*, *Saccharopolyspora* and *Bacillus clausii* in PC tissues is positively associated with $CD8^+$ T-cell infiltration in the cancer and predicts long-term survival [3]. Thus, cancer microbiota in PC patients may help modify the immune status of the tumor microenvironment and metabolize anticancer drugs. In this study, *Microbacterium* and *Stenotrophomonas* were detected in PC tissues. Both genera were also detected in PC

tissues in previous reports [3, 5], but the roles of both genera in the tumor microenvironment are unknown. Interestingly, both genera formed complex networks with fecal and oral microbes. Cancer *Stenotrophomonas* strongly co-occurred with fecal *Bifidobacterium adolescentis*, which was negatively correlated with cancer stage. To manipulate the cancer microbiota to modify the tumor microenvironment, scholars must determine whether alteration of members in the intestinal or oral microbiota affects the cancer microbiota and how to change the network between the cancer, fecal and oral microbiota.

In conclusion, species-level dysbiosis occurred in the gut microbiota of PC patients. Moreover, dysbiotic gut microbiota in PC patients formed complex networks with oral and cancer microbiota, and gut bacterial species abundant in the PC patients were closely linked with poor prognostic factors in the network. These results regarding dysbiotic microbes might contribute to establishing non-invasive fecal or salivary diagnostic markers to detect early PCs or predict prognosis and contribute to generating strategies to manipulate microbial networks, including cancer bacteria.

Acknowledgements

We thank Traci Raley, MS, ELS, from Edanz Group (https://en-author-services.edanzgroup.com/ac) for editing a draft of this manuscript.

Disclosure of conflict of interest

None.

Address correspondence to: Dr. Eishiro Mizukoshi, Department of Gastroenterology, Graduate School of Medical Sciences, Kanazawa University, Kanazawa, Ishikawa 920-8641, Japan. Tel: +81-76-265-2233; Fax: +81-76-234-4250; E-mail: eishirom@m-kanazawa.jp

References

[1] Siegel RL, Miller KD and Jemal A. Cancer statistics, 2020. CA Cancer J Clin 2020; 70: 7-30.

[2] Yamaguchi K, Okusaka T, Shimizu K, Furuse J, Ito Y, Hanada K, Shimosegawa T and Soc JP. EBM-based Clinical guidelines for pancreatic cancer (2013) issued by the Japan pancreas society: a synopsis. Jpn J Clin Oncol 2014; 44: 883-888.

[3] Riquelme E, Zhang Y, Zhang L, Montiel M, Zoltan M, Dong W, Quesada P, Sahin I, Chandra V, San Lucas A, Scheet P, Xu H, Hanash SM, Feng L, Burks JK, Do KA, Peterson CB, Nejman D, Tzeng CD, Kim MP, Sears CL, Ajami N, Petrosino J, Wood LD, Maitra A, Straussman R, Katz M, White JR, Jenq R, Wargo J and McAllister F. Tumor microbiome diversity and composition influence pancreatic cancer outcomes. Cell 2019; 178: 795-806, e12.

[4] Geller LT, Barzily-Rokni M, Danino T, Jonas OH, Shental N, Nejman D, Gavert N, Zwang Y, Cooper ZA, Shee K, Thaiss CA, Reuben A, Livny J, Avraham R, Frederick DT, Ligorio M, Chatman K, Johnston SE, Mosher CM, Brandis A, Fuks G, Gurbatri C, Gopalakrishnan V, Kim M, Hurd MW, Katz M, Fleming J, Maitra A, Smith DA, Skalak M, Bu J, Michaud M, Trauger SA, Barshack I, Golan T, Sandbank J, Flaherty KT, Mandinova A, Garrett WS, Thayer SP, Ferrone CR, Huttenhower C, Bhatia SN, Gevers D, Wargo JA, Golub TR and Straussman R. Potential role of intratumor bacteria in mediating tumor resistance to the chemotherapeutic drug gemcitabine. Science 2017; 357: 1156-1160.

[5] Pushalkar S, Hundeyin M, Daley D, Zambirinis CP, Kurz E, Mishra A, Mohan N, Aykut B, Usyk M, Torres LE, Werba G, Zhang K, Guo Y, Li Q, Akkad N, Lall S, Wadowski B, Gutierrez J, Kochen Rossi JA, Herzog JW, Diskin B, Torres-Hernandez A, Leinwand J, Wang W, Taunk PS, Savadkar S, Janal M, Saxena A, Li X, Cohen D, Sartor RB, Saxena D and Miller G. The pancreatic cancer microbiome promotes oncogenesis by induction of innate and adaptive immune suppression. Cancer Discov 2018; 8: 403-416.

[6] Thomas RM, Gharaibeh RZ, Gauthier J, Beveridge M, Pope JL, Guijarro MV, Yu Q, He Z, Ohland C, Newsome R, Trevino J, Hughes SJ, Reinhard M, Winglee K, Fodor AA, Zajac-Kaye M and Jobin C. Intestinal microbiota enhances pancreatic carcinogenesis in preclinical models. Carcinogenesis 2018; 39: 1068-1078.

[7] Thomas RM and Jobin C. Microbiota in pancreatic health and disease: the next frontier in microbiome research. Nat Rev Gastroenterol Hepatol 2020; 17: 53-64.

[8] Ren ZG, Jiang JW, Xie HY, Li A, Lu HF, Xu SY, Zhou L, Zhang H, Cui GY, Chen XH, Liu YX, Wu LM, Qin N, Sun RR, Wang W, Li LJ, Wang WL and Zheng SS. Gut microbial profile analysis by MiSeq sequencing of pancreatic carcinoma patients in China. Oncotarget 2017; 8: 95176-95191.

[9] Michaud DS, Izard J, Wilhelm-Benartzi CS, You DH, Grote VA, Tjonneland A, Dahm CC, Overvad K, Jenab M, Fedirko V, Boutron-Ruault MC, Clavel-Chapelon F, Racine A, Kaaks R, Boeing H, Foerster J, Trichopoulou A, Lagiou P, Tricho-

poulos D, Sacerdote C, Sieri S, Palli D, Tumino R, Panico S, Siersema PD, Peeters PHM, Lund E, Barricarte A, Huerta JM, Molina-Montes E, Dorronsoro M, Quiros JR, Duell EJ, Ye WM, Sund M, Lindkvist B, Johansen D, Khaw KT, Wareham N, Travis RC, Vineis P, Bueno-de-Mesquita HB and Riboli E. Plasma antibodies to oral bacteria and risk of pancreatic cancer in a large European prospective cohort study. Gut 2013; 62: 1764-1770.

[10] Half E, Keren N, Reshef L, Dorfman T, Lachter I, Kluger Y, Reshef N, Knobler H, Maor Y, Stein A, Konikoff FM and Gophna U. Fecal microbiome signatures of pancreatic cancer patients. Sci Rep 2019; 9: 16801.

[11] Schmieder R and Edwards R. Quality control and preprocessing of metagenomic datasets. Bioinformatics 2011; 27: 863-864.

[12] Caporaso JG, Kuczynski J, Stombaugh J, Bittinger K, Bushman FD, Costello EK, Fierer N, Pena AG, Goodrich JK, Gordon JI, Huttley GA, Kelley ST, Knights D, Koenig JE, Ley RE, Lozupone CA, McDonald D, Muegge BD, Pirrung M, Reeder J, Sevinsky JR, Turnbaugh PJ, Walters WA, Widmann J, Yatsunenko T, Zaneveld J and Knight R. QIIME allows analysis of high-throughput community sequencing data. Nat Methods 2010; 7: 335-336.

[13] Langmead B and Salzberg SL. Fast gapped-read alignment with Bowtie 2. Nat Methods 2012; 9: 357-359.

[14] Li H, Handsaker B, Wysoker A, Fennell T, Ruan J, Homer N, Marth G, Abecasis G and Durbin R; 1000 Genome Project Data Processing Subgroup. The sequence alignment/map format and SAMtools. Bioinformatics 2009; 25: 2078-2079.

[15] Segata N, Waldron L, Ballarini A, Narasimhan V, Jousson O and Huttenhower C. Metagenomic microbial community profiling using unique clade-specific marker genes. Nat Methods 2012; 9: 811-814.

[16] Abubucker S, Segata N, Goll J, Schubert AM, Izard J, Cantarel BL, Rodriguez-Mueller B, Zucker J, Thiagarajan M, Henrissat B, White O, Kelley ST, Methe B, Schloss PD, Gevers D, Mitreva M and Huttenhower C. Metabolic reconstruction for metagenomic data and its application to the human microbiome. PLoS Comput Biol 2012; 8: e1002358.

[17] Buchfink B, Xie C and Huson DH. Fast and sensitive protein alignment using DIAMOND. Nat Methods 2015; 12: 59-60.

[18] Rampelli S, Soverini M, Turroni S, Quercia S, Biagi E, Brigidi P and Candela M. ViromeScan: a new tool for metagenomic viral community profiling. BMC Genomics 2016; 17: 165.

[19] Segata N, Izard J, Waldron L, Gevers D, Miropolsky L, Garrett WS and Huttenhower C. Metagenomic biomarker discovery and explanation. Genome Biol 2011; 12: R60.

[20] Iida N, Mizukoshi E, Yamashita T, Terashima T, Arai K, Seishima J and Kaneko S. Overuse of antianaerobic drug is associated with poor postchemotherapy prognosis of patients with hepatocellular carcinoma. Int J Cancer 2019; 145: 2701-2711.

[21] Seishima J, Iida N, Kitamura K, Yutani M, Wang Z, Seki A, Yamashita T, Sakai Y, Honda M, Yamashita T, Kagaya T, Shirota Y, Fujinaga Y, Mizukoshi E and Kaneko S. Gut-derived Enterococcus faecium from ulcerative colitis patients promotes colitis in a genetically susceptible mouse host. Genome Biol 2019; 20: 252.

[22] Edgar RC. Search and clustering orders of magnitude faster than BLAST. Bioinformatics 2010; 26: 2460-2461.

[23] DeSantis TZ, Hugenholtz P, Larsen N, Rojas M, Brodie EL, Keller K, Huber T, Dalevi D, Hu P and Andersen GL. Greengenes, a chimera-checked 16S rRNA gene database and workbench compatible with ARB. Appl Environ Microbiol 2006; 72: 5069-5072.

[24] Shannon P, Markiel A, Ozier O, Baliga NS, Wang JT, Ramage D, Amin N, Schwikowski B and Ideker T. Cytoscape: a software environment for integrated models of biomolecular interaction networks. Genome Res 2003; 13: 2498-2504.

[25] Gao J, Tarcea VG, Karnovsky A, Mirel BR, Weymouth TE, Beecher CW, Cavalcoli JD, Athey BD, Omenn GS, Burant CF and Jagadish HV. Metscape: a Cytoscape plug-in for visualizing and interpreting metabolomic data in the context of human metabolic networks. Bioinformatics 2010; 26: 971-973.

[26] Jackson MA, Goodrich JK, Maxan ME, Freedberg DE, Abrams JA, Poole AC, Sutter JL, Welter D, Ley RE, Bell JT, Spector TD and Steves CJ. Proton pump inhibitors alter the composition of the gut microbiota. Gut 2016; 65: 749-756.

[27] Freedberg DE, Toussaint NC, Chen SP, Ratner AJ, Whittier S, Wang TC, Wang HH and Abrams JA. Proton pump inhibitors alter specific taxa in the human gastrointestinal microbiome: a crossover trial. Gastroenterology 2015; 149: 883-885, e889.

[28] Imhann F, Bonder MJ, Vich Vila A, Fu J, Mujagic Z, Vork L, Tigchelaar EF, Jankipersadsing SA, Cenit MC, Harmsen HJ, Dijkstra G, Franke L, Xavier RJ, Jonkers D, Wijmenga C, Weersma RK and Zhernakova A. Proton pump inhibitors affect the gut microbiome. Gut 2016; 65: 740-748.

[29] Iida N, Dzutsev A, Stewart CA, Smith L, Bouladoux N, Weingarten RA, Molina DA, Salcedo R, Back T, Cramer S, Dai RM, Kiu H, Cardone M, Naik S, Patri AK, Wang E, Marincola FM, Frank

KM, Belkaid Y, Trinchieri G and Goldszmid RS. Commensal bacteria control cancer response to therapy by modulating the tumor microenvironment. Science 2013; 342: 967-970.

[30] Iida N, Mizukoshi E, Yamashita T, Terashima T, Arai K, Seishima J and Kaneko S. Overuse of antianaerobic drug is associated with poor postchemotherapy prognosis of patients with hepatocellular carcinoma. Int J Cancer 2019; 145: 2701-2711.

[31] Birchenough GM, Nystrom EE, Johansson ME and Hansson GC. A sentinel goblet cell guards the colonic crypt by triggering Nlrp6-dependent Muc2 secretion. Science 2016; 352: 1535-1542.

[32] Venkatesh M, Mukherjee S, Wang HW, Li H, Sun K, Benechet AP, Qiu ZJ, Maher L, Redinbo MR, Phillips RS, Fleet JC, Kortagere S, Mukherjee P, Fasano A, Le Ven J, Nicholson JK, Dumas ME, Khanna KM and Mani S. Symbiotic bacterial metabolites regulate gastrointestinal barrier function via the xenobiotic sensor PXR and toll-like receptor 4. Immunity 2014; 41: 296-310.

[33] Brandl K, Plitas G, Mihu CN, Ubeda C, Jia T, Fleisher M, Schnabl B, DeMatteo RP and Pamer EG. Vancomycin-resistant enterococci exploit antibiotic-induced innate immune deficits. Nature 2008; 455: 804-U808.

[34] Nakamoto N, Sasaki N, Aoki R, Miyamoto K, Suda W, Teratani T, Suzuki T, Koda Y, Chu PS, Taniki N, Yamaguchi A, Kanamori M, Kamada N, Hattori M, Ashida H, Sakamoto M, Atarashi K, Narushima S, Yoshimura A, Honda K, Sato T and Kanai T. Gut pathobionts underlie intestinal barrier dysfunction and liver T helper 17 cell immune response in primary sclerosing cholangitis. Nat Microbiol 2019; 4: 492-503.

[35] Atarashi K, Suda W, Luo CW, Kawaguchi T, Motoo I, Narushima S, Kiguchi Y, Yasuma K, Watanabe E, Tanoue T, Thaiss CA, Sato M, Toyooka K, Said HS, Yamagami H, Rice SA, Gevers D, Johnson RC, Segre JA, Chen K, Kolls JK, Elinav E, Morita H, Xavier RJ, Hattori M and Honda K. Ectopic colonization of oral bacteria in the intestine drives T(H)1 cell induction and inflammation. Science 2017; 358: 359-365.

Supplementary Table 1. Baseline characteristics of the subjects

	HD (n=18)	Panc.Cancer (n=24)	*P*-value
Gender (M/F)*	7/11	14/10	0.212
Age (years)†	59.2 ± 13.7	66.9 ± 9.2	0.058
BMI (kg/m^2)†	21.1 ± 2.77	21.9 ± 1.75	0.129
WBC (/μl)†	5,596 ± 1,986	5,489 ± 1,455	0.825
CRP (mg/dl)†	0.09 ± 0.15	0.22 ± 0.31	0.055
Plasma glucose (mg/dl)†	87.5 ± 5.5	132.3 ± 45.6	0.0001
HbA1c (%)†	5.6 ± 0.3	6.9 ± 1.7	0.0012
CEA (mg/dl, range)	NA	3.4 (1-18.4)	NA
Stage (0/1a/1b/2a/2b/3/4)	NA	1/0/2/7/0/11/3	NA
PPI/H2RA (medicated/not medicated)*	0/18	10/14	0.0017
Current smoking (Yes/No)*	3/15	10/14	0.082

†, values are means ± SD. *, analyzed by Chi-squared test. Other values were analyzed by Mann-Whitney U test. Differences were considered significant for $P<0.05$. BMI, body mass index; CEA, carcinoembryonic antigen; CRP, C-reactive protein; HD, healthy donors; HbA1c, hemoglobin A1c; H2RA, H_2 receptor antagonist; NA, not available; PPI, proton-pump inhibitor; WBC, white blood cells.

Supplementary Table 2. Significant differential bacterial pathways in gut among pancreatic cancer patients and healthy donors

ko number	pathway name	pathway class	class	LDA_score	*p*-value
ko00121	Secondary bile acid biosynthesis	Metabolism; Lipid metabolism	HD	3.58680	0.03490
ko00290	Valine, leucine and isoleucine biosynthesis	Metabolism; Amino acid metabolism	HD	3.41416	0.00037
ko00300	Lysine biosynthesis	Metabolism; Amino acid metabolism	HD	2.96237	0.04743
ko00450	Selenocompound metabolism	Metabolism; Metabolism of other amino acids	HD	2.99857	0.04692
ko00564	Glycerophospholipid metabolism	Metabolism; Lipid metabolism	HD	3.09630	0.00007
ko00730	Thiamine metabolism	Metabolism; Metabolism of cofactors and vitamins	HD	3.37017	0.00149
ko00750	Vitamin B6 metabolism	Metabolism; Metabolism of cofactors and vitamins	HD	2.81613	0.04743
ko00770	Pantothenate and CoA biosynthesis	Metabolism; Metabolism of cofactors and vitamins	HD	2.87126	0.02369
ko00970	Aminoacyl-tRNA biosynthesis	Genetic Information Processing; Translation	HD	3.23765	0.00478
ko01051	Biosynthesis of ansamycins	Metabolism; Metabolism of terpenoids and polyketides	HD	3.87906	0.00654
ko01055	Biosynthesis of vancomycin group antibiotics	Metabolism; Metabolism of terpenoids and polyketides	HD	3.73390	0.02217
ko02030	Bacterial chemotaxis	Cellular Processes; Cell motility	HD	3.52583	0.02045
ko02040	Flagellar assembly	Cellular Processes; Cell motility	HD	3.45294	0.00952
ko03010	Ribosome	Genetic Information Processing; Translation	HD	3.45731	0.00605
ko03018	RNA degradation	Genetic Information Processing; Folding, sorting and degradation	HD	2.66457	0.01575
ko04626	Plant-pathogen interaction	Organismal Systems; Environmental adaptation	HD	2.74390	0.00761
ko00040	Pentose and glucuronate interconversions	Metabolism; Carbohydrate metabolism	Panc.Cancer	3.00604	0.01186
ko00051	Fructose and mannose metabolism	Metabolism; Carbohydrate metabolism	Panc.Cancer	3.09910	0.01469
ko00053	Ascorbate and aldarate metabolism	Metabolism; Carbohydrate metabolism	Panc.Cancer	2.87023	0.01092
ko00061	Fatty acid biosynthesis	Metabolism; Lipid metabolism	Panc.Cancer	3.07413	0.03952
ko00130	Ubiquinone and other terpenoid-quinone biosynthesis	Metabolism; Metabolism of cofactors and vitamins	Panc.Cancer	2.78997	0.00320
ko00140	Steroid hormone biosynthesis	Metabolism; Lipid metabolism	Panc.Cancer	2.73176	0.00031
ko00280	Valine, leucine and isoleucine degradation	Metabolism; Amino acid metabolism	Panc.Cancer	3.07125	0.00011
ko00310	Lysine degradation	Metabolism; Amino acid metabolism	Panc.Cancer	2.66277	0.01546
ko00311	Penicillin and cephalosporin biosynthesis	Metabolism; Biosynthesis of other secondary metabolites	Panc.Cancer	2.76193	0.00150
ko00360	Phenylalanine metabolism	Metabolism; Amino acid metabolism	Panc.Cancer	2.72420	0.00915
ko00440	Phosphonate and phosphinate metabolism	Metabolism; Metabolism of other amino acids	Panc.Cancer	2.76729	0.00271
ko00472	D-Arginine and D-ornithine metabolism	Metabolism; Metabolism of other amino acids	Panc.Cancer	2.84577	0.01837
ko00510	N-Glycan biosynthesis	Metabolism; Glycan biosynthesis and metabolism	Panc.Cancer	2.88173	0.00165
ko00511	Other glycan degradation	Metabolism; Glycan biosynthesis and metabolism	Panc.Cancer	3.54547	0.00100
ko00520	Amino sugar and nucleotide sugar metabolism	Metabolism; Carbohydrate metabolism	Panc.Cancer	2.82468	0.00193
ko00531	Glycosaminoglycan degradation	Metabolism; Glycan biosynthesis and metabolism	Panc.Cancer	3.24806	0.00158
ko00540	Lipopolysaccharide biosynthesis	Metabolism; Glycan biosynthesis and metabolism	Panc.Cancer	3.29105	0.00249
ko00626	Naphthalene degradation	Metabolism; Xenobiotics biodegradation and metabolism	Panc.Cancer	2.98865	0.01425
ko00650	Butanoate metabolism	Metabolism; Carbohydrate metabolism	Panc.Cancer	3.07053	0.03067
ko00720	Carbon fixation pathways in prokaryotes	Metabolism; Energy metabolism	Panc.Cancer	3.37313	0.00054

ko00785	Lipoic acid metabolism	Metabolism; Metabolism of cofactors and vitamins	Panc.Cancer	3.33545	0.00149
ko00790	Folate biosynthesis	Metabolism; Metabolism of cofactors and vitamins	Panc.Cancer	3.17760	0.00347
ko00908	Zeatin biosynthesis	Metabolism; Metabolism of terpenoids and polyketides	Panc.Cancer	2.65240	0.02369
ko00910	Nitrogen metabolism	Metabolism; Energy metabolism	Panc.Cancer	2.76259	0.00442
ko00983	Drug metabolism-other enzymes	Metabolism; Xenobiotics biodegradation and metabolism	Panc.Cancer	3.54574	0.01503
ko03410	Base excision repair	Genetic Information Processing; Replication and repair	Panc.Cancer	2.66944	0.01809
ko04141	Protein processing in endoplasmic reticulum	Genetic Information Processing; Folding, sorting and degradation	Panc.Cancer	2.68504	0.01455
ko04974	Protein digestion and absorption	Organismal Systems; Digestive system	Panc.Cancer	2.65326	0.00259

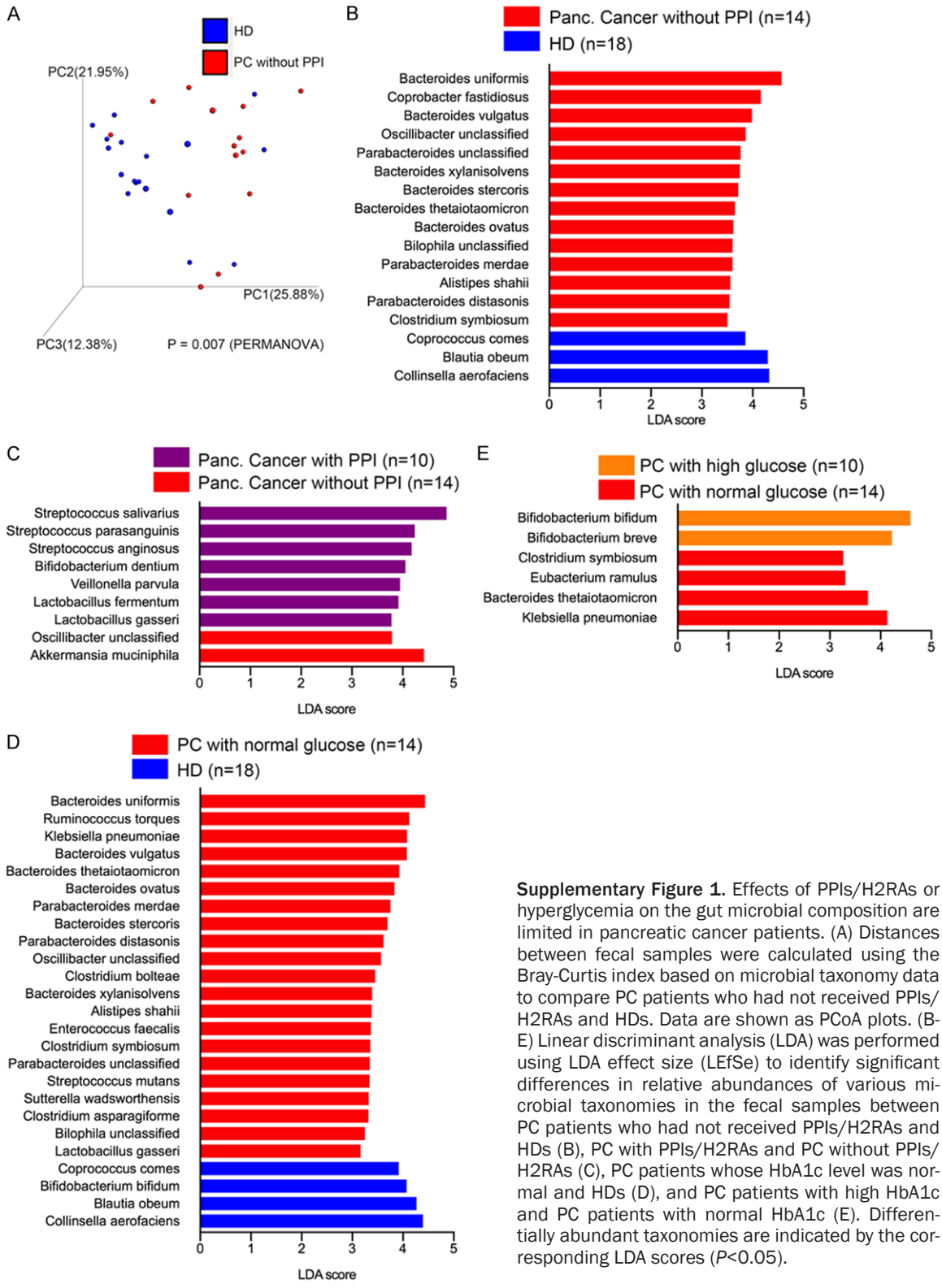

Supplementary Figure 1. Effects of PPIs/H2RAs or hyperglycemia on the gut microbial composition are limited in pancreatic cancer patients. (A) Distances between fecal samples were calculated using the Bray-Curtis index based on microbial taxonomy data to compare PC patients who had not received PPIs/H2RAs and HDs. Data are shown as PCoA plots. (B-E) Linear discriminant analysis (LDA) was performed using LDA effect size (LEfSe) to identify significant differences in relative abundances of various microbial taxonomies in the fecal samples between PC patients who had not received PPIs/H2RAs and HDs (B), PC with PPIs/H2RAs and PC without PPIs/H2RAs (C), PC patients whose HbA1c level was normal and HDs (D), and PC patients with high HbA1c and PC patients with normal HbA1c (E). Differentially abundant taxonomies are indicated by the corresponding LDA scores (P<0.05).

Supplementary Table 3. Treatments for pancreatic cancers

Treatments	Number of patients
surgery	5
surgery after chemotherapy	6
chemotehrapy	9
radiation therapy	2
chemoradiation therapy	2

Supplementary Table 4. Hazard ratio of death in pancreatic cancer patients analyzed by Cox proportional hazard model

Factors	Univariate *P*-value	Hazard ratio of death
age	0.251	1.065
gender female	0.693	0.71
BMI	0.89	0.978
PPI Yes	0.049	8.715
cancer stage	0.026	3.646
serum CEA	0.018	1.979
blood WBC counts	0.851	1
serum Amylase	0.103	0.97
HbA1c	0.464	0.761
Smoking Yes	0.354	0.447
Alcohol Yes	0.788	0.792
feces_Acidaminococcus_unclassified	0.525	0.186
feces_Akkermansia_muciniphila	0.539	0.793
feces_Alistipes_onderdonkii	0.767	1.072
feces_Alistipes_putredinis	0.718	1.085
feces_Alistipes_shahii	0.645	1.401
feces_Anaerostipes_hadrus	0.383	0.062
feces_Bacteroidales_bacterium_ph8	0.469	0.159
feces_Bacteroides_caccae	0.065	1.299
feces_Bacteroides_cellulosilyticus	0.144	5.01
feces_Bacteroides_coprocola	0.206	1.324
feces_Bacteroides_dorei	0.485	0.848
feces_Bacteroides_eggerthii	0.624	1.062
feces_Bacteroides_finegoldii	0.529	3.023
feces_Bacteroides_fragilis	0.739	0.766
feces_Bacteroides_ovatus	0.052	1.461
feces_Bacteroides_plebeius	0.43	0.673
feces_Bacteroides_stercoris	0.766	0.937
feces_Bacteroides_thetaiotaomicron	0.931	1.018
feces_Bacteroides_uniformis	0.35	0.906
feces_Bacteroides_vulgatus	0.135	1.195
feces_Bacteroides_xylanisolvens	0.831	1.093
feces_Barnesiella_intestinihominis	0.719	1.274
feces_Bifidobacterium_adolescentis	0.354	0.692
feces_Bifidobacterium_animalis	0.012	1.65
feces_Bifidobacterium_bifidum	0.503	0.842
feces_Bifidobacterium_dentium	0.73	0.891

feces_Bifidobacterium_longum	0.683	0.922
feces_Bifidobacterium_pseudocatenulatum	0.46	1.378
feces_Bilophila_unclassified	0.248	2.483
feces_Clostridium_bartlettii	0.816	0.107
feces_Clostridium_bolteae	0.765	0.709
feces_Clostridium_hathewayi	0.814	0.807
feces_Clostridium_nexile	0.566	0.112
feces_Clostridium_ramosum	0.808	0.582
feces_Clostridium_symbiosum	0.572	1.696
feces_Collinsella_aerofaciens	0.018	2.455
feces_Coprobacillus_unclassified	0.685	0.922
feces_Coprococcus_catus	0.387	0.008
feces_Coprococcus_comes	0.899	1.477
feces_Dialister_invisus	0.461	0.196
feces_Dorea_formicigenerans	0.122	1.862
feces_Dorea_longicatena	0.506	0.709
feces_Eggerthella_lenta	0.671	0.638
feces_Eggerthella_unclassified	0.44	0.559
feces_Escherichia_coli	0.464	0.849
feces_Escherichia_unclassified	0.523	0.652
feces_Eubacterium_eligens	0.174	1.688
feces_Eubacterium_hallii	0.949	0.981
feces_Eubacterium_ramulus	0.094	7.451
feces_Eubacterium_rectale	0.29	0.688
feces_Eubacterium_ventriosum	0.009	71.33
feces_Faecalibacterium_prausnitzii	0.549	1.064
feces_Flavonifractor_plautii	0.579	0
feces_Klebsiella_pneumoniae	0.046	1.117
feces_Lachnospiraceae_bacterium_1_1_57FAA	0.428	1.252
feces_Lachnospiraceae_bacterium_5_1_63FAA	0.386	5.643
feces_Lachnospiraceae_bacterium_8_1_57FAA	0.816	1.322
feces_Lactobacillus_fermentum	0.09	2.469
feces_Lactobacillus_gasseri	0.269	2.683
feces_Lactobacillus_salivarius	0.101	1.119
feces_Megamonas_unclassified	0.828	0.991
feces_Oscillibacter_unclassified	0.244	0.486
feces_Parabacteroides_distasonis	0.281	0.349
feces_Parabacteroides_goldsteinii	0.678	0.618
feces_Parabacteroides_merdae	0.903	1.034
feces_Parabacteroides_unclassified	0.593	0.004
feces_Paraprevotella_unclassified	0.445	1.518
feces_Phascolarctobacterium_succinatutens	0.28	1.485
feces_Roseburia_hominis	0.775	0.162
feces_Roseburia_intestinalis	0.03	62.757
feces_Roseburia_inulinivorans	0.178	1.43
feces_Roseburia_unclassified	0.751	0.184
feces_Ruminococcus_bromii	0.335	0.915
feces_Ruminococcus_gnavus	0.627	1.023
feces_Ruminococcus_obeum	0.071	2.025
feces_Ruminococcus_torques	0.801	1.038
feces_Streptococcus_anginosus	0.709	1.025

feces_Streptococcus_australis	0.555	0.465
feces_Streptococcus_gordonii	0.854	1.465
feces_Streptococcus_mutans	0.913	1.039
feces_Streptococcus_parasanguinis	0.546	1.044
feces_Streptococcus_salivarius	0.834	1.01
feces_Streptococcus_thermophilus	0.022	3.286
feces_Streptococcus_tigurinus	0.781	987.254
feces_Streptococcus_vestibularis	0.157	1.956
feces_Subdoligranulum_unclassified	0.852	0.973
feces_Sutterella_wadsworthensis	0.669	0.547
feces_Veillonella_parvula	0.636	0.876
feces_Veillonella_unclassified	0.579	0.181
tumor_Microbacterium	NA	NA
tumor_Stenotrophomonas	NA	NA
saliva_Abiotrophia_defectiva	0.312	1.654
saliva_Actinomyces_graevenitzii	0.207	1.306
saliva_Actinomyces_odontolyticus	0.817	0.621
saliva_Actinomyces_oris	0.943	0.838
saliva_Actinomyces_viscosus	0.87	0.74
saliva_Alloprevotella_tannerae	0.784	1.118
saliva_Alloscardovia_omnicolens	0.769	1.102
saliva_Atopobium_parvulum	0.6	0.581
saliva_Campylobacter_concisus	0.067	3.95
saliva_Capnocytophaga_gingivalis	0.09	6.478
saliva_Capnocytophaga_unclassified	0.095	2.374
saliva_Corynebacterium_durum	0.091	24447.608
saliva_Corynebacterium_matruchotii	0.532	0.717
saliva_Fusobacterium_nucleatum	0.455	0.56
saliva_Fusobacterium_periodonticum	0.505	1.118
saliva_Gemella_haemolysans	0.873	1.062
saliva_Gemella_morbillorum	0.438	0.177
saliva_Gemella_sanguinis	0.764	1.072
saliva_Granulicatella_adiacens	0.114	0.062
saliva_Granulicatella_elegans	0.442	15.921
saliva_Granulicatella_unclassified	0.212	0.452
saliva_Haemophilus_parainfluenzae	0.878	0.988
saliva_Haemophilus_sputorum	0.474	0.153
saliva_Human_herpesvirus_4	0.324	1.379
saliva_Lachnospiraceae_bacterium_oral_taxon_082	0.966	0.827
saliva_Lautropia_mirabilis	0.946	0.997
saliva_Leptotrichia_unclassified	0.9	0.613
saliva_Leptotrichia_wadei	0.856	0.184
saliva_Megasphaera_micronuciformis	0.956	1.016
saliva_Neisseria_flavescens	0.742	0.89
saliva_Neisseria_meningitidis	0.429	0.191
saliva_Neisseria_sicca	0.066	45.016
saliva_Neisseria_unclassified	0.713	0.969
saliva_Oribacterium_sinus	0.387	1.173
saliva_Parvimonas_unclassified	0.589	1.545
saliva_Peptostreptococcus_stomatis	0.289	715.019
saliva_Peptostreptococcus_unclassified	0.403	1.864
saliva_Porphyromonas_endodontalis	0.494	0.718

saliva_Porphyromonas_gingivalis	0.855	0.975
saliva_Porphyromonas_sp_oral_taxon_279	0.682	0.976
saliva_Prevotella_denticola	0.502	1.586
saliva_Prevotella_histicola	0.883	1.009
saliva_Prevotella_melaninogenica	0.508	1.04
saliva_Prevotella_nanceiensis	0.303	0.59
saliva_Prevotella_nigrescens	0.483	1.447
saliva_Prevotella_oris	0.59	0.401
saliva_Prevotella_oulorum	0.502	0
saliva_Prevotella_pallens	0.241	1.321
saliva_Prevotella_salivae	0.64	0.757
saliva_Prevotella_veroralis	0.45	2.513
saliva_Rothia_aeria	0.08	1.513
saliva_Rothia_dentocariosa	0.457	1.082
saliva_Rothia_mucilaginosa	0.611	1.009
saliva_Rothia_unclassified	0.426	0.343
saliva_Solobacterium_moorei	0.972	0.958
saliva_Stomatobaculum_longum	0.798	1.163
saliva_Streptococcus_anginosus	0.953	0.947
saliva_Streptococcus_australis	0.235	1.184
saliva_Streptococcus_gordonii	0.743	3.016
saliva_Streptococcus_infantis	0.541	0.888
saliva_Streptococcus_mitis_oralis_pneumoniae	0.58	0.951
saliva_Streptococcus_parasanguinis	0.319	0.933
saliva_Streptococcus_salivarius	0.228	0.81
saliva_Streptococcus_sanguinis	0.332	1.071
saliva_Streptococcus_tigurinus	0.621	0.64
saliva_Streptococcus_vestibularis	0.551	0.587
saliva_Veillonella_atypica	0.726	0.967
saliva_Veillonella_dispar	0.283	1.507
saliva_Veillonella_parvula	0.855	0.979
saliva_Veillonella_unclassified	0.64	1.051
feces_ko00121	0.754	1
feces_ko00290	0.492	1
feces_ko00300	0.758	1
feces_ko00450	0.682	1
feces_ko00564	0.075	1.002
feces_ko00730	0.388	1
feces_ko00750	0.738	1
feces_ko00770	0.148	1
feces_ko00970	0.877	1
feces_ko01051	0.992	1
feces_ko01055	0.466	1
feces_ko02030	0.72	1
feces_ko02040	0.545	1
feces_ko03010	0.576	1
feces_ko03018	0.132	0.999
feces_ko04626	0.816	1
feces_ko00040	0.465	1
feces_ko00051	0.497	1
feces_ko00053	0.397	1
feces_ko00061	0.456	1

feces_ko00130	0.397	1.001
feces_ko00140	0.509	0.999
feces_ko00280	0.097	0.998
feces_ko00310	0.124	1.002
feces_ko00311	0.182	0.999
feces_ko00360	0.615	1
feces_ko00440	0.668	1.001
feces_ko00472	0.127	1
feces_ko00510	0.62	0.998
feces_ko00511	0.168	1
feces_ko00520	0.935	1
feces_ko00531	0.112	1
feces_ko00540	0.056	1
feces_ko00626	0.498	1
feces_ko00650	0.149	1.001
feces_ko00720	0.07	0.999
feces_ko00785	0.569	1
feces_ko00790	0.286	1
feces_ko00908	0.426	1
feces_ko00910	0.17	0.999
feces_ko00983	0.137	1
feces_ko03410	0.339	0.999
feces_ko04141	0.359	0.997
feces_ko04974	0.119	0.996
Alloherpesviridae; Cyprinivirus	0.702	111.492
Baculoviridae; Alphabaculovirus	0.419	15279.567
Baculoviridae; Betabaculovirus	0.699	8.63E+28
Flaviviridae; Hepacivirus	0.425	97773025
Herpesviridae; Cytomegalovirus	0.57	1329077.58
Herpesviridae; Macavirus	0.633	1.02E+33
Herpesviridae; Muromegalovirus	0.504	0
Herpesviridae; Proboscivirus	0.263	9.22E+15
Herpesviridae; Simplexvirus	0.365	2.67E+11
Herpesviridae; Varicellovirus	0.784	0
Iridoviridae; Iridovirus	0.066	9.22E+15
Mimiviridae; Unclassified	0.504	0
Nimaviridae; Whispovirus	0.481	0
Nudiviridae; Unclassified	0.548	0
Partitiviridae; Alphapartitivirus	0.391	0
Partitiviridae; Betapartitivirus	0.636	0
Phycodnaviridae; Chlorovirus	0.657	6.31E+15
Phycodnaviridae; Coccolithovirus	0.568	0
Phycodnaviridae; Phaeovirus	0.91	1.00E-03
Phycodnaviridae; Prymnesiovirus	0.072	9.22E+15
Phycodnaviridae; Unclassified	0.785	1.44E+03
Picornaviridae; Cardiovirus	0.419	5.467
Polydnaviridae; Bracovirus	0.371	0
Polydnaviridae; Ichnovirus	0.542	2.68E+06
Poxviridae; Avipoxvirus	0.361	0
Poxviridae; Betaentomopoxvirus	0.794	0
Poxviridae; Cervidpoxvirus	0.349	1.33E+09
Poxviridae; Orthopoxvirus	0.631	0

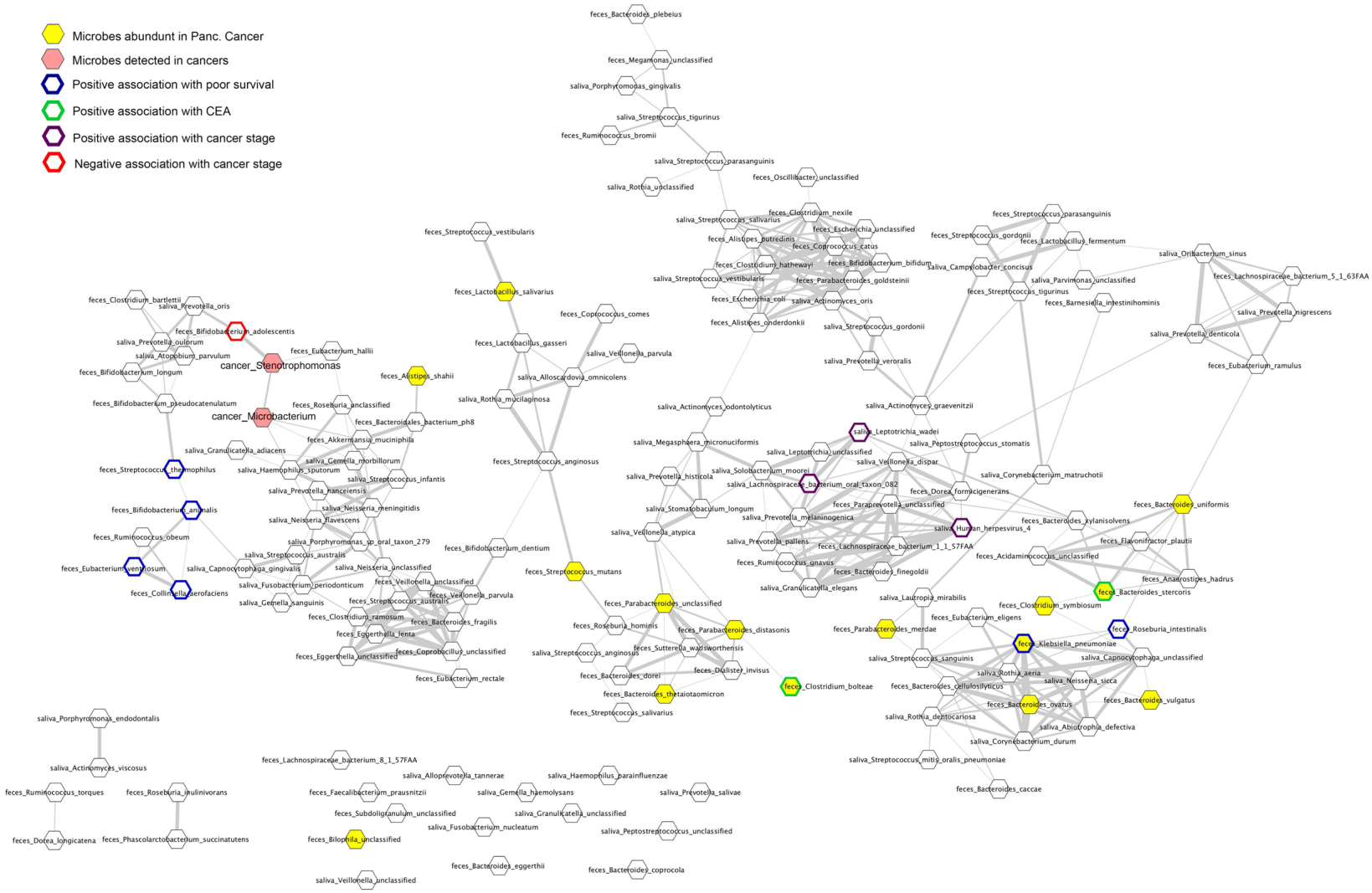

Supplementary Figure 2. Gut microbiota compositions of pancreatic cancer patients are highly associated with oral microbiota. Pearson correlation was calculated between relative abundances of fecal and salivary microbes in PC patients and shown as networks. Correlations coefficients ≥0.7 are shown as edges. Nodes of fecal microbes abundant in PC patients compared with HDs are highlighted in yellow. Nodes of cancer microbes are highlighted in pink. Positive association with a poor prognosis based on the increased hazard of death, blue border; positive association with serum CEA level, green border; positive association with cancer stage, purple border; #, negative association with cancer stage, red border.

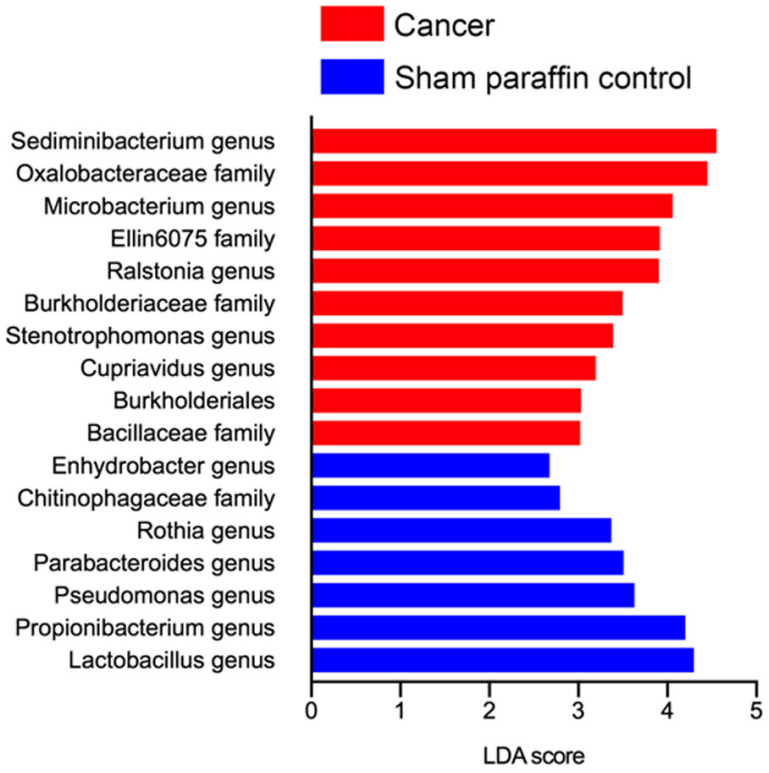

Supplementary Figure 3. Bacteria was detected in pancreatic cancer tissues. Linear discriminant analysis (LDA) was performed using LDA effect size (LEfSe) to identify significant differences in relative microbial abundances between cancer tissues and sham paraffin controls. Differentially abundant taxonomies are indicated by the corresponding LDA scores ($P<0.05$).